trans-[Ru(NO)(NH_3)P(O^-)($OEt)_2$]$^{2+}$: A new and robust NO/HNO-donor in aqueous media

Daniela R. Truzzi, Douglas W. Franco

PII: S0020-1693(14)00285-0
DOI: http://dx.doi.org/10.1016/j.ica.2014.05.010
Reference: ICA 15992

To appear in: *Inorganica Chimica Acta*

Received Date: 14 February 2014
Revised Date: 21 April 2014
Accepted Date: 9 May 2014

Please cite this article as: D.R. Truzzi, D.W. Franco, *trans*-[Ru(NO)(NH_3)P(O^-)($OEt)_2$]$^{2+}$: A new and robust NO/HNO-donor in aqueous media, *Inorganica Chimica Acta* (2014), doi: http://dx.doi.org/10.1016/j.ica.2014.05.010

trans-[Ru(NO)(NH_3)P(O^-)($OEt)_2$]$^{2+}$: A new and robust NO/HNO-donor in aqueous media

Daniela R. Truzzi[a]; Douglas W. Franco[a]*

[a] Departamento de Química e Física Molecular, Instituto de Química de São Carlos, Universidade de São Paulo, Av. Trabalhador São-carlense, 400, Centro, São Carlos, São Paulo, Brazil.

*Address inquiries to this author, email: douglas@iqsc.usp.br

Keywords: Ruthenium complex / Nitric oxide / Nitroxyl / Phosphite

Abstract

This study describes the synthesis and reactivity in aqueous media of a new potential NO/HNO-donor: *trans*-[Ru(NO)(NH_3)$_4$P(O^-)($OEt)_2$]($PF_6)_2$. This compound exhibits a remarkable robustness over a wide range of pH relative to other similar ruthenium phosphorus nitrosyl complexes. At pH 3.0 and 25°C, *trans*-[Ru(NO)(NH_3)$_4$P(O^-)($OEt)_2$]($PF_6)_2$ decays, yielding free diethyl phosphite with a half-life of 9 days ($k = 8.9 \times 10^{-7}$ s^{-1}). At pH 7.5 and 25°C, this complex is competitively consumed by diethyl phosphite dissociation ($k = 5.15 \times 10^{-5}$ s^{-1}) and nucleophilic attack at the nitrosyl group ($k = 7.25 \times 10^{-5}$ s^{-1}). Nevertheless, the *trans*-[Ru(NO)(NH_3)$_4$P(O^-)($OEt)_2$]($PF_6)_2$ exhibits a half-life of 1.5 h (pH 7.5 and 25°C) for delivering NO/HNO by electrochemical activation at potentials of -0.50 and -0.80 V *vs* SCE. The NO liberation from *trans*-[Ru(NO)(NH_3)$_4$P(O^-)($OEt)_2$]$^+$ ion occurs with $k_{-NO} = 0.24 \pm 0.01$ s^{-1}, and electrochemical data indicate that $k_{-HNO} >> k_{-NO}$.

1. Introduction

Ruthenium nitrosyl complexes of the type *trans*-$[Ru(NO)(NH_3)_4L]^{3+}$ are a promising nitric oxide donor (NO-donor) platform [1, 2]. *In vitro* and *in vivo* tests have successfully established their activity in the hippocampus [3], aorta rings [4-6] and against Chagas disease [7-9], *Leishmania major* [10] and cancer cells [11]. Among the tested compounds are those in which L = 4-pic, py, pz, im*N*, im*C*, nic, ina and $P(OEt)_3$ [2, 6, 7, 9-12]. Their biological activity is attributed to their NO-donor ability upon reduction, which can be modulated through the judicious choice of L. Phosphorus(III) ligands, such as phosphites ($P(OR)_3$) and phosphines ($P(R)_3$) are interesting due to their high *trans* effect and *trans* influence [12-15] properties, which can tune the reduction potential ($E_{NO^+/NO}$) and the specific rate constant for NO liberation (k_{-NO}) of the NO^+ fragment in these nitrosyl complexes [4, 5, 14]. Furthermore, due to the possibility of varying the nature of R, additional tuning of the phosphorus atom σ and π donor/acceptor abilities and the complex solubility can be achieved.

For example, *trans*-$[Ru(NO)(NH_3)_4P(OEt)_3](PF_6)_3$ exhibits $E_{NO^+/NO}$ = -0.24 V *vs* SCE and k_{-NO} = 0.97 s^{-1} [14], characteristics that are relevant for situations in which fast nitric oxide liberation is required. In addition, after NO-donation, the resulting complex ion *trans*-$[Ru(H_2O)(NH_3)_4P(OEt)_3]^{2+}$ is able to react with nitrite (NO_2^-) and, through an acid-base equilibrium, convert NO_2^- into NO^+ ligand [16], renewing the NO source. This system would be very interesting in hypoxic conditions, where oxygen-dependent NO synthases may be inhibited, by providing an alternative pathway for the production of nitric oxide through nitrite conversion [17]. It is interesting to recall that nitrite is present in plasma at an average concentration of 114±11 nmol L^{-1} [18], and the reduction potential of the $[RuNO]^{3+}$ fragment is accessible to biological reductors [9, 10, 14].

Despite the interesting characteristics of *trans*-$[Ru(NO)(NH_3)_4P(OEt)_3](PF_6)_3$ as a NO-donor, it is not stable for practical application in biological media (pH ≥ 5) due to nucleophilic attack at the triethyl phosphite ligand and at the nitrosonium group [19], decreasing the NO-donation efficiency of this compound.

Recently, phosphorous acid (the simplest phosphite) was chosen as a probe in which nucleophilic attack on the phosphite molecule is avoided by the absence of carbon chains [20]. In this case, the *trans*-$[Ru(NO)(NH_3)_4P(O^-)(OH)_2]^{2+}$ undergoes isomerization promoted by the nitrosyl group, yielding *trans*-$[Ru(NO)(NH_3)_4(O)P(OH)_2]^{2+}$ and *trans*-$[Ru(NO)(NH_3)_4(O)P(H)(OH)_2]^{3+}$ ions in aqueous media. This isomerization reaction also would reduce the compound NO-donor efficiency [20].

Therefore, this work presents a synthesis and reactivity study in aqueous media of the new *trans*-$[Ru(NO)(NH_3)_4P(O^-)(OEt)_2](PF_6)_2$ complex. Diethyl phosphite is an interesting alternative to the phosphorus(III) ligand because, unlike triethyl phosphite and phosphorous acid, it maintains both the dissociable proton (hydroxyl group) and the ethyl groups (electron donors).

2. Experimental Section

2.1 Chemicals and reagents

All chemicals were of analytical grade (Sigma-Aldrich, Strem or Merck). Ruthenium trichloride ($RuCl_3 \cdot 3H_2O$) was the starting reagent for the synthesis of the ruthenium nitrosyl complex described herein. The solvents were purified following literature procedures [21]. All syntheses and manipulations were carried out under an argon atmosphere [22].

2.2 Synthesis of the complexes

The *trans*-$[Ru(NH_3)_5Cl](Cl)_2$ [23] and *trans*-$[Ru(H_2O)(NH_3)_5](PF_6)_2$ [24] complexes were synthetized according to literature procedures.

2.2.1 trans-$[Ru(NO)(NH_3)_4P(O^-)(OEt)_2](PF_6)_2$ synthesis

First, 3.4×10^{-4} mol of *trans*-$[Ru(H_2O)(NH_3)_5](PF_6)_2$ (169 mg) and 3.9×10^{-4} mol of diethyl phosphite (0.5 mL) were added into 15 mL of argon-degassed acetone. After 1 h, NO was bubbled into the solution for 4 h. Next, the acetone was evaporated, and 100 mg of NH_4PF_6 and 50 mL of ether/ethanol (10:1) were added. The light red solid obtained was separated through filtration, dried and stored under vacuum and the absence of light.

Yield: 40%.

Theoretical elemental analysis for *trans*-$[Ru(NO)(NH_3)_4P(O^-)(OEt)_2](PF_6)_2 \cdot 1/2CH_3CH_2OH$: C 9.25, H 3.88 and N 11.09. Found: C 9.23, H 3.71 and N 11.05.

2.3 Instruments

UV-vis spectra were acquired using a Hitachi U-3501 instrument, 1.0-5.0 cm quartz cells and a thermostatic bath at 25 ± 0.1°C.

Infrared spectra were obtained using a Bomem-102 instrument using KBr pellets (32 scans) for solid analysis and a silicon window with a 0.05-mm Teflon spacer (8 scans) for solutions at a resolution of ±2 cm^{-1}.

Cyclic voltammetry (CV) and differential pulse voltammetry (DPV) were performed in a Princeton Applied Research 264A instrument. The electrochemical cell was composed of a saturated calomel electrode (SCE), a platinum plate and a glassy carbon electrode as the reference, auxiliary and working electrodes, respectively.

The specific rate constant for NO liberation (k_{-NO}) was calculated using the Nicholson and Shain electrochemical method [25] at pH 2.0, μ = 0.1 mol L^{-1} and 25 ± 0.1°C. Considering the NO dissociation from *trans*-$[Ru(NO)(NH_3)_4L]^{n+}$ fragments as a charge

transfer followed by an irreversible chemical reaction, the specific rate constant for the NO liberation (k_{-NO}) was calculated based in the I_{pa}/I_{pc} ratio with the scan rate variation [25]. The slope of the plot of $k.\tau$ (obtained from the working curve [25]) versus τ gives the k_{-NO} value.

NMR spectra were acquired in a Agilent 500/54 Premium Shielded instrument using a 5-mm probe and 3-(trimethylsilyl)-2,2',3,3'-tetradeuteropropionic acid (TMSP-D4) ($\delta_{1H,13C}$ = 0 ppm) or NH_4PF_6 salt (δ_{31P} = -144 ppm) as internal references and D_2O as the solvent. All of the solutions were degassed using argon, their pH and strength ionic were controlled. For the solutions at pH 7.5, tris(hydroxymethyl)aminomethane (TRIS) buffer was used. Unless otherwise noted, trifluoroacetic acid (HTFA) was employed for pH adjustment.

2.4 Kinetic measurements

The *trans*-$[Ru(NO)(NH_3)_4P(O^-)(OEt)_2]^{2+}$ ions were analysed in aqueous medium at pH 3.0 and 7.5 using ^{31}P NMR, UV-vis and IR. All experiments were carried out at 25°C. The data were modelled as a first-order reaction, with k being estimated from $\ln(A-A_t)$ *vs* time.

2.5 Computational details

The Gaussian03 [26] package was used to perform the calculations. The Kohn–Sham density functional theory (DFT) [27] with the Becke three-parameter hybrid exchange-correlation functional (B3LYP) and the standard DGAUSS basis set (DGDZVP for Ru, DGDZVP2 for P and DGTZVP for H, C, N and O) was used to carry out the molecular geometry optimizations [28, 29]. Symmetry conditions were not imposed [30]. The IEPCM model of solvation with water as the solvent was used [31-33]. The vibrational frequencies were carried out using the same method and the basis set under the keyword freq and did not exhibited imaginary frequencies indicating a true minimum. The orbital population was obtained from pop = full keyword and the electronic spectra were obtained using the TD-DFT

calculation as implemented in the Gaussian03 package. The NBO 3.0 programme implemented in the Gaussian03 package [34, 35] was used for natural bond orbital calculations. For all of the structures calculated herein, the orientation is as follows: the (NO)–Ru–($P(OH)(OEt)_2$) vector is the z-axis, and the x and y-axis correspond to the H_3N–Ru–NH_3 vectors.

3. Results and Discussion

3.1 Trans-$[Ru(NO)(NH_3)_4P(O^-)(OEt)_2](PF_6)_2$ characterization

Trans-$[Ru(NO)(NH_3)_4P(O^-)(OEt)_2](PF_6)_2$ was isolated as an EPR-silent orange solid. The orbital composition for this complex showed that the HOMO is 94% localized in Ru (d_{xy}) and the LUMO+0,1 are composed of 23% Ru (d_{xz}, d_{yz}) and 74% NO (p_x, p_y; π^*). The Ru-N=O angle obtained from DFT calculations is 175°, which strongly suggests that the NO ligand has nitrosonium character [2].

The $[Ru(NO)]^{3+}$ fragment exhibits a Ru(II) metal center with Ru(III) character. Indeed, the pK_a for water and phosphorous acid molecules in *trans*-$[Ru(NO)(H_2O)(salen)]^+$ (pK_a = 4.50) [36] and *trans*-$[Ru(NO)(NH_3)_4(P(OH)_3)]^{3+}$ (pK_a = 0.74) [20] are slightly smaller than those in the respective aqua-ruthenium(III) complexes: *trans*-$[Ru(H_2O)_2(salen)]^+$ (pK_a = 5.90) [36] and *trans*-$[Ru(H_2O)(NH_3)_4(P(OH)_3)]^{3+}$ (pK_a = 1.0) [37]. Thus, the pK_a for diethyl phosphite molecule in *trans*-$[Ru(NO)(NH_3)_4P(OH)(OEt)_2]^{3+}$ is estimated to be of the same order of magnitude as that in *trans*-$[Ru(H_2O)(NH_3)_4P(OH)(OEt)_2]^{3+}$ (pK_a = 1.5) [37]. According to UV-vis experiments (Fig. 1S), a band enlargement with an increase of absorbance at 270 and 360 nm and, a small blue shift of $\Delta = 4$ nm are observed when the solution pH changes from 1.0 to 3.0. This could be an indicative of the diethyl phosphite ligand deprotonation which would occurs at pH higher than 2.0, but it does not

enable an accurate pK_a calculation. Therefore, in this study, in aqueous medium at pH > 2.0, the diethyl phosphite in *trans*-$[Ru(NO)(NH_3)_4P(O^-)(OEt)_2]^{2+}$ will be depicted in its deprotonated form because it will certainly be the dominant form present under these conditions.

The electronic spectrum of *trans*-$[Ru(NO)(NH_3)_4P(O^-)(OEt)_2]^{2+}$ in solution at pH 2.0, μ = 0.1 mol L^{-1} (Fig. 2S), similarly to those observed for other compounds of the *trans*-$[Ru(NO)(NH_3)_4L]X_n$ series [38, 39], exhibited bands at λ ~ 530 nm (ε ~ 20 L mol^{-1} cm^{-1}), 310 nm (ε = 956 L mol^{-1} cm^{-1}) and 242 nm (ε = 1509 L mol^{-1} cm^{-1}).

According to TD-DFT calculations, the absorption at 530 nm is assigned to the metal-ligand charge transfer (MLCT) HOMO(d_{xy}Ru) ➔ LUMO+0,1(π*NO), while the 310 nm band would be a mixture of ligand-ligand charge transfer (LLCT), ($P(O^-)(OEt)_2$)HOMO-1 ➔ LUMO+0,1(π*NO) and MLCT HOMO-3,4(d_{xz},d_{yz}Ru) ➔ LUMO(π*NO). The most intense band at 242 nm is mainly composed by an LLCT ($P(O^-)(OEt)_2$)HOMO-2,5 ➔ LUMO+0,1(π*NO) and a d-d transition of the HOMO-3,4(d_{xz},d_{yz}Ru) ➔ LUMO+2,3($d_{z2}d_{x2-y2}$Ru) type.

Although the diethyl phosphite ligand presents a dissociable proton, the infrared spectra of the nitrosyl complex of diethyl phosphite in the solid state (KBr) and in aqueous medium (hydrogen ion concentration of 2.0 mol L^{-1} to 10^{-8} mol L^{-1}) exhibited just one νNO^+ at 1887 cm^{-1}. This is different from the observations for the protonated and deprotonated forms of *trans*-$[Ru(NO)(NH_3)_4P(OH)_3]^{3+}$/*trans*-$[Ru(NO)(NH_3)_4P(O^-)(OH)_2]^{2+}$ ions, which exhibit two νNO^+ (1892 and 1879 cm^{-1}), one for each species [20]. The DFT calculation for the structures *trans*-$[Ru(NO)(NH_3)_4P(OH)(OEt)_2]^{3+}$ and *trans*-$[Ru(NO)(NH_3)_4P(O^-)(OEt)_2]^{2+}$ yielded NO^+ frequencies at 1893 and 1883 cm^{-1}, respectively. These values are similar to one another, suggesting the possibility of band overlap in the experimental spectra. Indeed, the plot of both theoretical ν_{NO+} presented a

bandwidth at half-maximum ($w_{1/2}$) of 22 cm^{-1}, which is the same value observed experimentally for ν_{NO+} = 1887 cm^{-1} in the title complex (Fig. 3S).

The ^{31}P NMR spectra for *trans*-$[Ru(NO)(NH_3)_4P(O^-)(OEt)_2]^{2+}$ obtained in solution from 2.0 mol L^{-1} HTFA until reaching pH 7.5 exhibited just one singlet at 68 ppm (Table 1). This single chemical shift is different from that observed when phosphorous acid ($P(OH)_3$) is bonded to $[Ru(NO)(NH_3)_4]^{3+}$. In the last case, a singlet at 68 ppm for the protonated form and a singlet at 60 ppm for the deprotonated form can be observed [20]. However, for the diethyl complex, the NBO charges from DFT calculations show that the charge on the phosphorus atom does not change substantially after the deprotonation of *trans*-$[Ru(NO)(NH_3)_4P(OH)(OEt)_2]^{3+}$ (1.150) to form *trans*-$[Ru(NO)(NH_3)_4P(O^-)(OEt)_2]^{2+}$ (1.158), thus corroborating the experimental data. Table 1 shows the ^1H, ^{13}C and ^{31}P NMR data for *trans*-$[Ru(NO)(NH_3)_4P(O^-)(OEt)_2]^{2+}$ in D_2O.

Insert Table 1

The cyclic voltammograms for solutions containing *trans*-$[Ru(NO)(NH_3)_4P(O^-)(OEt)_2]^{2+}$ are depicted in Fig. 1a. The nitrosonium ligand is reduced at E_{cp} = -0.50 V *vs* SCE (reaction 1), and the nitric oxide ligand is then reduced at E_{cp} = -0.80 V *vs* SCE (reaction 2). Considering that the pK_a for HNO molecule in *trans*-$[Ru(HNO)(NH_3)_4P(OEt)_3]^{2+}$ estimated from DFT calculations is 9.9 [40] and $P(O^-)(OEt)_2$ exhibits a π-acidity less than that of $P(OEt)_3$ [12], in *trans*-$[Ru(HNO)(NH_3)_4P(O^-)(OEt)_2]^{2+}$, the HNO molecule probably exhibits $pK_a \geq 10$. Thus, in solutions with pH < 10, the second reduction process (reaction 2) would yield *trans*-$[Ru(HNO)(NH_3)_4P(O^-)(OEt)_2]^{2+}$ instead of *trans*-$[Ru(NO^-)(NH_3)_4P(O^-)(OEt)_2]^{+}$. The NO/NO^+ and HNO/NO oxidation waves are only partially observed in Fig. 1a at E_{ap} = -0.42 V

and E_{ap} = -0.63 V *vs* SCE due to the high *trans* effect of the phosphite ligand, which leads to a fast NO/HNO dissociation. The reversible couple observed at 0.29 V *vs* SCE is attributed to the Ru^{III}/Ru^{II} couple in the aqua complex (reaction 3).

$$trans\text{-}[Ru(NO^{+})(NH_3)_4P(O^{-})(OEt)_2]^{2+} \underset{-e^-}{\overset{+e^-}{\rightleftharpoons}} trans\text{-}[Ru(NO)(NH_3)_4P(O^{-})(OEt)_2]^{+} \quad (1)$$

$$trans\text{-}[Ru(NO)(NH_3)_4P(O^{-})(OEt)_2]^{+} \underset{-e^-}{\overset{+e^-}{\rightleftharpoons}} trans\text{-}[Ru(HNO)(NH_3)_4P(O^{-})(OEt)_2]^{+} \quad (2)$$

$$trans\text{-}[Ru(H_2O)(NH_3)_4P(O^{-})(OEt)_2]^{2+} \underset{-e^-}{\overset{+e^-}{\rightleftharpoons}} trans\text{-}[Ru(H_2O)(NH_3)_4P(O^{-})(OEt)_2]^{+} \quad (3)$$

Insert Figure 1

Applying the approach of Nicholson and Shain [25], the k_{-NO} value for *trans*-$[Ru(NO)(NH_3)_4P(O^{-})(OEt)_2]^{+}$ ion was calculated as 0.24 ± 0.01 s^{-1} at pH 2.0 and 25 ± 0.1°C (Fig. 4S). This value is four times smaller than the value measured for *trans*-$[Ru(NO)(NH_3)_4P(OEt)_3]^{2+}$ (k_{-NO} = 0.97 s^{-1} [14]). The k_{-HNO} (the specific rate constant for nitroxyl liberation) for this complex was not calculated using the Nicholson and Shain [25] method because the oxidation process of the coordinated HNO was not clearly observed, even at 5°C and a high scan rate (2 V s^{-1}), which indicates that $k_{-HNO} >> k_{-NO}$ for *trans*-$[Ru(NO)(NH_3)_4P(O^{-})(OEt)_2](PF_6)_2$ complex.

The HNO dimerizes to N_2O ($k_{dim} = 8 \times 10^6$ M^{-1} s^{-1} [41]) in aqueous medium. Thus the N_2O identification [40] (E_{cp} = -0.32 V at pH 5.0 [42]) in solution, after one electron reduction of *trans*-$[Ru(NO)(NH_3)_4P(O^{-})(OEt)_2]^{+}$, can be a good indication of the HNO presence The Fig. 2 shows the differential pulse voltammetric experiments carried out using a N_2O saturated solution and a solution containing *trans*-$[Ru(NO)(NH_3)_4P(O^{-})(OEt)_2]^{2+}$ at 2.5 ±

0.1°C and pH 5.0 (the N_2O detection is pH dependent) before and after electrode polarization at -1.0 V. The E_{cp} = -0.32 V observed in N_2O saturated solution is similar to the one observed in the solution containing *trans*-$[Ru(NO)(NH_3)_4P(O^-)(OEt)_2]^{2+}$ indicating the release of HNO in solution and its consequent dimerization into N_2O.

Insert Figure 2

3.2 Aqueous medium stability of trans-$[Ru(NO)(NH_3)_4P(O^-)(OEt)_2]^{2+}$

Trans-$[Ru(NO)(NH_3)_4P(O^-)(OEt)_2]^{2+}$ was monitored at pH 3.0 using ^{31}P NMR. The ^{31}P NMR spectra initially exhibited just one peak at 68 ppm, which decayed (reaction 4) with $k = 8.90 \times 10^{-7}$ s^{-1} ($t_{1/2}$ = 9 days), yielding as the main product free diethyl phosphite and its hydrolysed products (15-0 ppm), which were formed with $t_{1/2}$ = 8.6 days.

$$\underset{\delta_{31P} = 68 \text{ ppm}}{\textit{trans}\text{-}[Ru(NO)(NH_3)_4P(O^-)(OEt)_2]^{2+}} \xrightarrow[25°C]{\text{pH 3.0}} \textit{trans}\text{-}[Ru(NO)(NH_3)_4(OH_2)]^{3+} + \underset{\delta_{31P} = 15\text{-}0 \text{ ppm}}{P(O^-)(OEt)_2} \quad (4)$$

Two peaks of very low intensity at 66 and 62 ppm were also observed, corresponding to *trans*-$[Ru(NO)(NH_3)_4P(OH)_2(OEt)]^{3+}$ and *trans*-$[Ru(NO)(NH_3)_4P(O^-)(OH)_2]^{2+}$, respectively. However, as judged from the product distribution analysis, the main reaction is the diethyl phosphite dissociation (reaction 4) and not the phosphite ligand hydrolysis.

According to ^{31}P NMR kinetic data obtained at pH 3.0 and 25 ± 0.1°C, *trans*-$[Ru(NO)(NH_3)_4P(O^-)(OEt)_2]^{2+}$ ($t_{1/2}$ = 9 days) is at least 3 times more stable than *trans*-$[Ru(NO)(NH_3)_4P(OEt)_3]^{3+}$ ($t_{1/2}$ = 2.8 days) [43] and 269 times more stable than *trans*-$[Ru(NO)(NH_3)_4P(O^-)(OH)_2]^{2+}$ ($t_{1/2}$ = 47.7 min) [20].

However, the behaviour of *trans*-$[Ru(NO)(NH_3)_4P(O^-)(OEt)_2]^{2+}$ in aqueous media does not match that observed for the corresponding nitrosyl complexes of triethyl phosphite [43] or phosphorous acid [20] under the same experimental conditions. *Trans*-$[Ru(NO)(NH_3)_4P(OEt)_3]^{3+}$ undergoes phosphorous ligand hydrolysis, whereas the *trans*-$[Ru(NO)(NH_3)_4P(O^-)(OH)_2]^{2+}$ isomerizes to the O-bonded compound (*trans*-$[Ru(NO)(NH_3)_4(O)P(OH)_2]^{2+}$) and only then undergoes phosphorus ligand dissociation [20]. On the other hand, the diethyl phosphite in *trans*-$[Ru(NO)(NH_3)_4P(O^-)(OEt)_2]^{2+}$ neither hydrolyses nor isomerizes but dissociates as is. This probably occurs due to the combination of the σ-inductive effect of the ethyl groups, which are absent in phosphorous acid, and the dissociable proton, which is absent in triethyl phosphite, which results in an extra negative charge over the phosphorus ligand, decreasing the hydrolysis and isomerization reaction rates and favouring the dissociation.

Considering that *trans*-$[Ru(NO)(NH_3)_4P(O^-)(OEt)_2]^{2+}$ is potentially useful as a NO/HNO-donor in biological media, the stability of this complex was also monitored as a function of time at pH 7.5 (TRIS buffer) by ^{31}P NMR, IR and UV-vis spectroscopy as well as cyclic voltammetry.

Fig. 3 shows the time course of the ^{31}P NMR chemical shift areas for *trans*-$[Ru(NO)(NH_3)_4P(O^-)(OEt)_2]^{2+}$ at pH 7.5 and 25 ± 0.5°C. The decay and formation profile shown in Fig. 3 is not trivial, indicating that consecutive and/or competitive reactions are taking place.

Insert Figure 3

Assuming first-order kinetic behaviour, the observed rate constants (k) of the decays and formations of each δ_{31P} in Fig. 3 can be obtained by plotting ln $(A-A_t)$ versus time (s).

In the time range of 0 to 7,000 s, the *trans*-$[Ru(NO)(NH_3)_4P(O^-)(OEt)_2]^{2+}$ peak at 68 ppm decays, yielding peaks at 15-0 ppm, corresponding to free diethyl phosphite and its hydrolysed products ($k_{f(15\text{-}0\ ppm)total} = 1.14 \times 10^{-4}\ s^{-1}$), and a peak at 138 ppm ($k_{f(138\ ppm)} = 7.50 \times 10^{-5}\ s^{-1}$).

After 7,000 s, the peak at 138 ppm decays, yielding a peak at 136 ppm ($k_{f(136\ ppm)} = 7.45 \times 10^{-5}\ s^{-1}$). This last peak also decays, yielding free diethyl phosphite and its hydrolysed products ($k_{f(15\text{-}0ppm)2} = 6.25 \times 10^{-5}\ s^{-1}$).

After 7,000 s, only the species at 136 ppm is able to generate free diethyl phosphite in solution, with $k_{f(15\text{-}0ppm)2} = 6.25 \times 10^{-5}\ s^{-1}$. However, within the first 7,000 s, free diethyl phosphite is produced at a rate of $k_{f(15\text{-}0ppm)total} = 1.14 \times 10^{-4}\ s^{-1}$, indicating that during this period, free diethyl phosphite is produced not only from the species at 136 ppm but also from the initial species at 68 ppm. Thus, the rate of the dissociation of diethyl phosphite from *trans*-$[Ru(NO)(NH_3)_4P(O^-)(OEt)_2]^{2+}$ can be estimated as $k_{f(15\text{-}0ppm)1} = 5.15 \times 10^{-5}\ s^{-1}$ from $k_{f(15\text{-}0ppm)1} = k_{f(15\text{-}0ppm)total} - k_{f(15\text{-}0ppm)2}$.

The peaks at 68 ppm and 15-0 ppm, as described above, are known to correspond to *trans*-$[Ru(NO)(NH_3)_4P(O^-)(OEt)_2]^{2+}$ and $P(OH)(OEt)_2$ and its hydrolysed species, respectively. This is not the case for the peaks at 138 and 136 ppm. To identify these species, *trans*-$[Ru(H_2O)(NH_3)_4P(O^-)(OEt)_2](PF_6)$ was synthesized, and the ^{31}P NMR spectra of the pH 7.5 solution containing this complex were obtained.

The ^{31}P NMR spectrum of *trans*-$[Ru(H_2O)(NH_3)_4P(O^-)(OEt)_2](PF_6)$ at pH 7.5 exhibited just one peak at 138 ppm. This peak diminishes as a function of time, yielding the peak at 136 ppm. Thus, the peak at 136 ppm probably corresponds to the complex product of diethyl phosphite ligand hydrolysis: *trans*-$[Ru(H_2O)(NH_3)_4P(O^-)(OH)(OEt)]^+$.

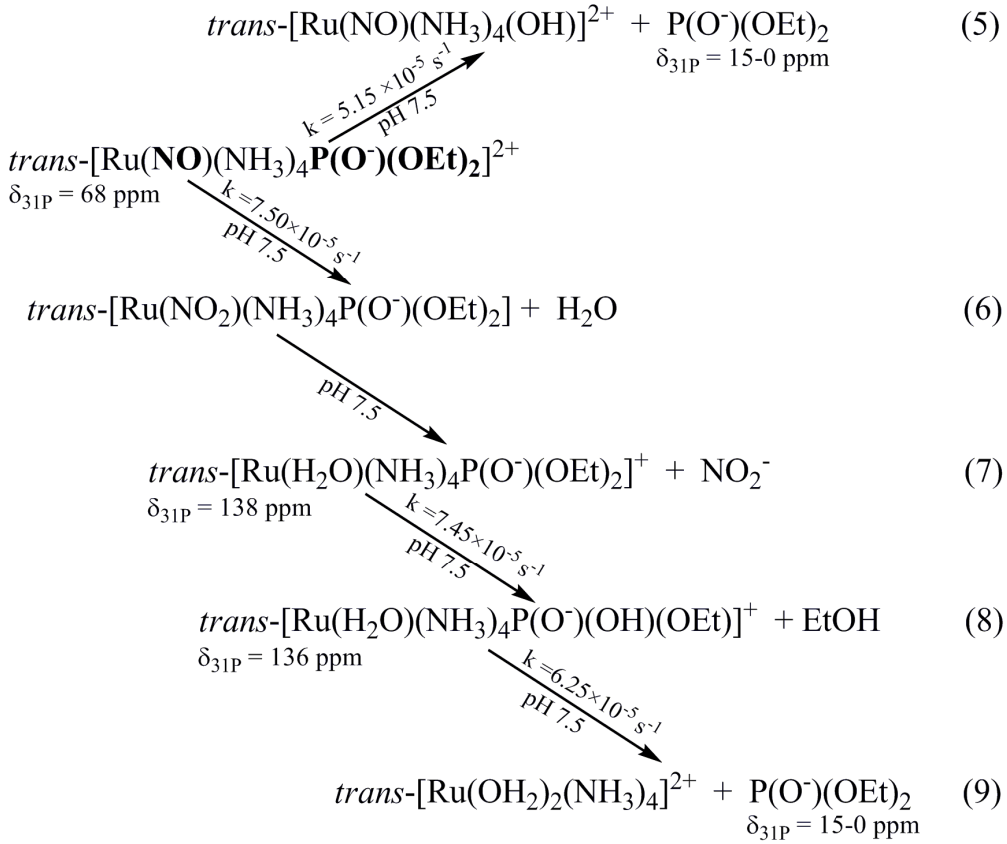

Therefore, in solution at pH 7.5, *trans*-$[Ru(NO)(NH_3)_4P(O^-)(OEt)_2]^{2+}$ (δ_{31P} = 68 ppm) is consumed competitively, yielding free diethyl phosphite (δ_{31P} = 15-0 ppm, reaction 5) and *trans*-$[Ru(H_2O)(NH_3)_4P(O^-)(OEt)_2]^+$ (δ_{31P} = 138 ppm, reaction 7). This last complex undergoes hydrolysis, giving rise to *trans*-$[Ru(H_2O)(NH_3)_4P(O^-)(OH)(OEt)]^+$ (δ_{31P} = 136 ppm, reaction 8), which also decays, yielding free diethyl phosphite (δ_{31P} = 15-0 ppm, reaction 9) as follows:

To produce *trans*-$[Ru(H_2O)(NH_3)_4P(O^-)(OEt)_2]^+$ (δ_{31P} = 138 ppm) from *trans*-$[Ru(NO)(NH_3)_4P(O^-)(OEt)_2]^{2+}$, a reaction centred on the nitrosonium ligand must occur. According to the literature [14, 16], at pH ≥ 5.0, the nitrosyl complex undergoes nucleophilic attack on the NO^+ group, yielding a nitrite complex. The formation of *trans*-$[Ru(NO_2)(NH_3)_4P(III)]^+$ can be indirectly determined spectrophotometrically through

the aquation of the nitrite ligand using pyrazine as an auxiliary ligand (reactions 10 and 11) [16].

$$trans\text{-}[Ru(NO_2)(NH_3)_4P(III)]^n + H_2O \rightleftharpoons trans\text{-}[Ru(H_2O)(NH_3)_4P(III)]^{n+1} + NO_2^- \quad (10)$$

$$trans\text{-}[Ru(H_2O)(NH_3)_4P(III)]^{n+1} + pz \rightleftharpoons trans\text{-}[Ru(pz)(NH_3)_4P(III)]^{n+1} + H_2O \quad (11)$$

Thus, the formation of the *trans*-$[Ru(pz)(NH_3)_4P(O^-)(OEt)_2]^+$ product (λ = 400 nm [37], Fig. 4) was followed in solution at pH 7.5 containing *trans*-$[Ru(NO)(NH_3)_4P(O^-)(OEt)_2]^{2+}$ and an excess of pyrazine. The initial nitrosyl complex was converted into *trans*-$[Ru(pz)(NH_3)_4P(O^-)(OEt)_2]^+$, and the observed rate constant (k) for nitrite aquation in *trans*-$[Ru(NO_2)(NH_3)_4P(O^-)(OEt)_2]$ at pH 7.5 and 25 ± 0.1°C was calculated as 1.19×10^{-4} s^{-1}.

Insert Figure 4

The same pH 7.5 solution containing *trans*-$[Ru(NO)(NH_3)_4P(O^-)(OEt)_2]^{2+}$ and an excess of pyrazine at 25 ± 0.1°C was also monitored by ^{31}P NMR. According to the spectra acquired as a function of time, *trans*-$[Ru(NO)(NH_3)_4P(O^-)(OEt)_2]^{2+}$ (δ_{31P} = 68 ppm) yields free diethyl phosphite (δ_{31P} = 15-0 ppm) and *trans*-$[Ru(pz)(NH_3)_4P(O^-)(OEt)_2]^+$ (δ_{31P} = 132 ppm) with $k_{f(132ppm)} = 1.18 \times 10^{-4}$ s^{-1}. This value is experimentally indistinguishable from that calculated using spectrophotometric data ($k = 1.19 \times 10^{-4}$ s^{-1}).

Trans-$[Ru(NO_2)(NH_3)_4P(O^-)(OEt)_2]$ species were not detected in the ^{31}P NMR spectra of pH 7.5 solutions containing *trans*-$[Ru(NO)(NH_3)_4P(O^-)(OEt)_2]^{2+}$. This absence is probably due to rapid nitrite complex consumption (reactions 7), which precludes *trans*-$[Ru(NO_2)(NH_3)_4P(O^-)(OEt)_2]$ accumulation.

The infrared spectra of *trans*-$[Ru(NO)(NH_3)_4P(O^-)(OEt)_2]^{2+}$ at pH 7.5 exhibited a decrease in ν_{NO+} = 1887 cm^{-1} (Fig. 5S) as function of time, which is also consistent with nitrosyl complex consumption.

The cyclic voltammograms of *trans*-$[Ru(NO)(NH_3)_4P(O^-)(OEt)_2]^{2+}$ at pH 7.5 and 25 ± 0.1°C initially exhibited a Ru(III)/Ru(II) couple at 0.15 V and the same reduction processes of NO^+/NO and NO/HNO (E = -0.50 and -0.80 V *vs* SCE). This observation indicates that this complex retains its ability to be activated through reduction and acts as a potential NO/HNO-donor at pH 7.5. With time, the current of these processes decreases, indicating again the consumption of the nitrosyl species.

It is interesting to note that the Ru(III)/Ru(II) couple in the *trans*-$[Ru(H_2O)(NH_3)_4P(O^-)(OEt)_2]^{2+}$/*trans*-$[Ru(H_2O)(NH_3)_4P(O^-)(OEt)_2]^{+}$ species is now (pH 7.5) shifted by +130 mV relative to the voltammogram obtained at pH 2.0 due to the diethyl phosphite deprotonation. Similar behaviour was observed when the ligand was phosphorous acid ($P(OH)_3$) [20], in which case the potential shifted by +120 mV.

Regarding nucleophilic attack on phosphite and on the nitrosyl group, the data collected suggest that *trans*-$[Ru(NO)(NH_3)_4P(O^-)(OEt)_2]^{2+}$ ($t_{1/2}$ = 1.5 h at pH 7.5 and 25 ± 0.5 °C) is the most robust among the *trans*-$[Ru(NO)(NH_3)_4P(III)]^{n+}$ complex ions studied to date [16, 20, 43]. The formation of *trans*-$[Ru(pz)(NH_3)_4P(O^-)(OEt)_2]^{+}$ from *trans*-$[Ru(NO)(NH_3)_4P(O^-)(OEt)_2]^{2+}$ at pH 7.5 ($k = 1.19 \times 10^{-4}$ s^{-1}) shows that the aquation rate of the nitrite ligand in *trans*-$[Ru(NO_2)(NH_3)_4P(O^-)(OEt)_2]$ is almost 100 times slower than that in *trans*-$[Ru(NO_2)(NH_3)_4P(OEt)_3]^{+}$ (1.30×10^{-2} s^{-1}) [44]. The increase in the stability of nitrite complex favours the *in vivo* catalytic cycle previously proposed [6, 9], in which the nitrite complex is converted into a nitrosyl complex [16], rebuilding the NO/HNO-donor complex.

Considering that there are several indications that NO molecules play an important role in pain modulation and can induce analgesia [45], *in vivo* tests using *trans*-$[Ru(NO)(NH_3)_4P(O^-)(OEt)_2]^{2+}$ as a NO/HNO-donor are being carried out. Preliminary results regarding anti-inflammatory effects indicate that 100 μmol kg^{-1} *trans*-$[Ru(NO)(NH_3)_4P(O^-)(OEt)_2]^{2+}$ considerably reduces the intensity of pain perception (hypernociception) in Swiss mice (Fig. 6S) [46].

4. Conclusions

Trans-$[Ru(NO)(NH_3)_4P(O^-)(OEt)_2](PF_6)_2$ is the first isolated example in the *trans*-$[Ru(NO)(NH_3)_4L]^{3+}$ series of a phosphorus ester of the type $P(OH)(OR)_2$ being bound to ruthenium center through the phosphorus atom.

The presence of both σ–inductor groups (P-O-R) and an acidic proton (P-O-H) bonded to the oxygen of phosphorus(III) precludes the hydrolysis and isomerization reactions on *trans*-$[Ru(NO)(NH_3)_4P(O^-)(OEt)_2]^{2+}$. In addition to being important in its own right and to the chemistry of phosphorous esters as ligands, the obtained information concerning how R/H groups modulate the phosphorus(III) ligand in terms of nucleophilic attack and isomerization reactions in the *trans*-$[Ru(NO)(NH_3)_4]^{3+}$ fragment will be helpful for better tailoring NO/HNO delivery systems.

Lastly, the data presented herein show that *trans*-$[Ru(NO)(NH_3)_4P(O^-)(OEt)_2]^{2+}$ is a fast NO/HNO-donor and is rather stable in aqueous media over a wide range of pH (pH 3.0 - 7.5). Thus, it is a potential alternative to the unstable *trans*-$[Ru(NO)(NH_3)_4P(OEt)_3]^{3+}$ and *trans*-$[Ru(NO)(NH_3)_4P(O^-)(OH)_2]^{2+}$ ion complexes.

Acknowledgments

The authors acknowledge FAPESP, CNPq and CAPES for financial support

5. References

[1] E. Tfouni, D.R. Truzzi, A. Tavares, A.J. Gomes, L.E. Figueiredo, D.W. Franco, Nitric Oxide, 26 (2012) 38-53.
[2] E. Tfouni, M. Krieger, B.R. McGarvey, D.W. Franco, Coord. Chem. Rev., 236 (2003) 57-69.
[3] A. Wieraszko, M.J. Clarke, D.R. Lang, L.G. Lopes, D.W. Franco, Life Sci., 68 (2001) 1535-1544.
[4] A.S. Torsoni, B.F. de Barros, J.C. Toledo, M. Haun, M.H. Krieger, E. Tfouni, D.W. Franco, Nitric Oxide, 6 (2002) 247-254.
[5] B.F. de Barros, J.C. Toledo, D.W. Franco, E. Tfouni, M.H. Krieger, Nitric Oxide, 7 (2002) 50-56.
[6] P.G. Zanichelli, H.F.G. Estrela, R.C. Spadari-Bratfisch, D.M. Grassi-Kassisse, D.W. Franco, Nitric Oxide, 16 (2007) 189-196.
[7] J.J. Silva, W.R. Pavanelli, J.C. Pereira, J.S. Silva, D.W. Franco, Antimicrob. Agents Ch., 53 (2009) 4414-4421.
[8] J.J.N. Silva, W.R. Pavanelli, F.R.S. Gutierrez, F.C.A. Lima, A.B.F. da Silva, J.S. Silva, D.W. Franco, J. Med. Chem., 51 (2008) 4104-4114.
[9] J.J. Silva, A.L. Osakabe, W.R. Pavanelli, J.S. Silva, D.W. Franco, Brit. J. Pharmacol., 152 (2007) 112-121.
[10] J.C.M. Pereira, V. Carregaro, D.L. Costa, J.S. da Silva, F.Q. Cunha, D.W. Franco, Eur. J. Med. Chem., 45 (2010) 4180-4187.
[11] R.Z. Osti, F.A. Serrano, T. Paschoalin, M. Massaoka, L.R. Travassos, D.R. Truzzi, E.G. Rodrigues, D.W. Franco, Aust. J. Chem., 65 (2012) 1333-1341.
[12] J.C. Toledo, B.D.S.L. Neto, D.W. Franco, Coordin Chem Rev, 249 (2005) 419-431.
[13] D.W. Franco, Coord. Chem. Rev., 119 (1992) 199-225.
[14] L.G.F. Lopes, E.E. Castellano, A.G. Ferreira, C.U. Davanzo, M.J. Clarke, D.W. Franco, Inorg. Chim. Acta, 358 (2005) 2883-2890.
[15] D.W. Franco, H. Taube, Inorg. Chem., 17 (1978) 571-578.
[16] R.Z. de Osti, D.W. Franco, Polyhedron, 26 (2007) 4746-4750.
[17] J.O. Lundberg, M.T. Gladwin, A. Ahluwalia, N. Benjamin, N.S. Bryan, A. Butler, P. Cabrales, A. Fago, M. Feelisch, P.C. Ford, B.A. Freeman, M. Frenneaux, J. Friedman, M. Kelm, C.G. Kevil, D.B. Kim-Shapiro, A.V. Kozlov, J.R. Lancaster, D.J. Lefer, K. McColl, K. McCurry, R.P. Patel, J. Petersson, T. Rassaf, V.P. Reutov, G.B. Richter-Addo, A. Schechter, S. Shiva, K. Tsuchiya, E.E. van Faassen, A.J. Webb, B.S. Zuckerbraun, J.L. Zweier, E. Weitzberg, Nat. Chem. Biol., 5 (2009) 865-869.
[18] P.H. MacArthur, S. Shiva, M.T. Gladwin, J. Chromatogr. B Analyt. Technol. Biomed. Life Sci., 851 (2007) 93-105.
[19] G. Metzker, J.C.T. Jr., F.C.A. Lima, A. Magalhães, D.R. Cardosoa, D.W. Franco, J. Braz. Chem. Soc., 21 (2010) 1266-1273.
[20] D.R. Truzzi, A.G. Ferreira, S.C. da Silva, E.E. Castellano, F.D. Chagas Alves Lima, D.W. Franco, Dalton Trans., 40 (2011) 12917-12925.
[21] D.D. Perrin, W. Almarge, L., D.P. Perrin, Purification of Laboratory Chemicals, Butterworth Heinemann, New York, 1983.
[22] D.F. Shriver, The manipulation of air-sensitive compounds, McGraw-Hill, New York, 1969.
[23] L.H. Vogt, J.L. Katz, S.E. Wiberley, Inorg. Chem., 4 (1965) 1157-1163.
[24] C.G. Kuehn, H. Taube, J. Am. Chem. Soc., 98 (1976) 689-702.
[25] R.S. Nicholson, I. Shain, Anal. Chem., 36 (1964) 706-723.

[26] M.J. Frisch, G.W. Trucks, H.B. Schlegel, G.E. Scuseria, M.A. Robb, J.R. Cheeseman, J.A. Montgomery Jr., T. Vreven, K.N. Kudin, J.C. Burant, J.M. Millam, S.S. Iyengar, J. Tomasi, V. Barone, B. Mennucci, M. Cossi, G. Scalmani, N. Rega, G.A. Petersson, H. Nakatsuji, M. Hada, M. Ehara, K. Toyota, R. Fukuda, J. Hasegawa, M. Ishida, T. Nakajima, Y. Honda, O. Kitao, H. Nakai, M. Klene, X. Li, J.E. Knox, H.P. Hratchian, J.B. Cross, V. Bakken, C. Adamo, J. Jaramillo, R. Gomperts, R.E. Stratmann, O. Yazyev, A.J. Austin, R. Cammi, C. Pomelli, J.W. Ochterski, P.Y. Ayala, K. Morokuma, G.A. Voth, P. Salvador, J.J. Dannenberg, V.G. Zakrzewski, S. Dapprich, A.D. Daniels, M.C. Strain, O. Farkas, D.K. Malick, A.D. Rabuck, K. Raghavachari, J.B. Foresman, J.V. Ortiz, Q. Cui, A.G. Baboul, S. Clifford, J. Cioslowski, B.B. Stefanov, G. Liu, A. Liashenko, P. Piskorz, I. Komaromi, R.L. Martin, D.J. Fox, T. Keith, M.A. Al-Laham, C.Y. Peng, A. Nanayakkara, M. Challacombe, P.M.W. Gill, B. Johnson, W. Chen, M.W. Wong, C. Gonzalez, J.A. Pople, Gaussian 03, Gaussian Inc, Wallingford CT, 2004.
[27] W. Kohn, L.J. Sham, Phys. Rev., 140 (1965) 1133-1138.
[28] A.D. Becke, J. Chem. Phys., 98 (1993) 1372-1377.
[29] C. Lee, W. Yang, R.G. Parr, Phys. Rev. B Condens. Matter, 37 (1988) 785-789.
[30] N. Godbout, D.R. Salahub, J. Andzelm, E. Wimmer, Can. J. Chem., 70 (1992) 560-571.
[31] E. Cances, B. Mennucci, J. Tomasi, J. Chem. Phys., 107 (1997) 3032-3041.
[32] A.E. Reed, L.A. Curtiss, F. Weinhold, Chem. Rev., 88 (1988) 899-926.
[33] A.E. Reed, F. Weinhold, J. Chem. Phys., 83 (1985) 1736-1740.
[34] W.R. Wadt, P.J. Hay, J. Chem. Phys., 82 (1985) 284-298.
[35] P.J. Hay, W.R. Wadt, J. Chem. Phys., 82 (1985) 299-310.
[36] J. Bordini, D.O. Novaes, I.E. Borissevitch, B.T. Owens, P.C. Ford, E. Tfouni, Inorg. Chim. Acta, 361 (2008) 2252-2258.
[37] R.L. Sernaglia, D.W. Franco, Inorg. Chem., 28 (1989) 3485-3489.
[38] R.M. Carlos, A.A. Ferro, H.A.S. Silva, M.G. Gomes, S.S.S. Borges, P.C. Ford, E. Tfouni, D.W. Franco, Inorg. Chim. Acta, 357 (2004) 1381-1388.
[[39] S.I. Gorelsky, S.C. da Silva, A.B.P. Lever, D.W. Franco, Inorg. Chim. Acta, 300 (2000) 698-708.
[40] G. Metzker, E.V. Stefaneli, J.C.M. Pereira, F.D.A. Lima, S.C. da Silva, D.W. Franco, Inorg. Chim. Acta, 394 (2013) 765-769.
[41] V. Shafirovich, S.V. Lymar, Proc. Natl. Acad. Sci. USA, 99 (2002) 7340-7345.
[42] B.X. Wang, X.Y. Li, Anal. Chem., 70 (1998) 2181-2187.
[43] D.R. Truzzi, D.W. Franco, Abstr. Pap. Am. Chem. Soc, 245 (2013).
[44] J.C. Toledo, in, University of Sao Paulo, São Carlos, PhD Thesis (2004).
[45] Y. Cury, G. Picolo, V.P. Gutierrez, S.H. Ferreira, Nitric Oxide, 25 (2011) 243-254.
[46] C.S. Freitas, A.C.R. Júnior, D.R. Truzzi, D.W. Franco, F.Q. Cunha, Manuscript in Preparation, (2014).

Figure Captions

Fig. 1. *Trans*-$[Ru(NO)(NH_3)_4P(O)(OEt)_2]^{2+}$ in aqueous solution at pH 2.0, μ = 0.1 mol L^{-1}, $C_{Ru} = 1.5 \times 10^{-3}$ mol L^{-1}, T = 5 ± 0.1°C. (a) Cyclic voltammogram obtained at a scan rate of 100 mV s^{-1}; (b) differential pulse voltammogram obtained at a scan rate of 10 mV s^{-1}.

Fig. 2. Differential pulse voltammograms at pH 5.0, μ = 0.1 mol L^{-1}, T = 2.5 ± 0.1°C and scan rate of 10 mV s^{-1}. Dotted line: DPV of *trans*-$[Ru(NO)(NH_3)_4P(O^-)(OEt)_2]^{2+}$ at $C_{Ru} = 3.0 \times 10^{-3}$ mol L^{-1}. Solid line: DPV of *trans*-$[Ru(NO)(NH_3)_4P(O^-)(OEt)_2]^{2+}$ at $C_{Ru} = 3.0 \times 10^{-3}$ mol L^{-1} after electrode polarization at -1.0 V. Dashed line: DPV of N_2O saturated solution.

Fig. 3. Product distribution as a function of time obtained from ^{31}P NMR kinetics data for *trans*-$[Ru(NO)(NH_3)_4P(O)(OEt)_2]^{2+}$ at pH 7.5 and 25 ± 0.5°C.
(a) δ_{31P} = 68 ppm; *trans*-$[Ru(NO)(NH_3)_4(P(O)(OEt)_2)]^{2+}$;
(b) δ_{31P} = 138 ppm; *trans*-$[Ru(OH)(NH_3)_4(P(O)(OEt)_2)]$;
(c) δ_{31P} = 136 ppm; *trans*-$[Ru(OH)(NH_3)_4(P(O)(OH)(OEt))]$;
(d) δ_{31P} = 15-0 ppm; $P(OH)(OEt)_2$ and its hydrolysed forms.

Fig. 4. Electronic spectra of *trans*-$[Ru(NO)(NH_3)_4P(O)(OEt)_2]^{2+}$ in an excess of pyrazine at pH 7.5 and 25 ± 0.1°C as a function of time. Inserted: $\ln(A-A_t)$ versus time (s); $R^2 = 0.997$.

Figure 1

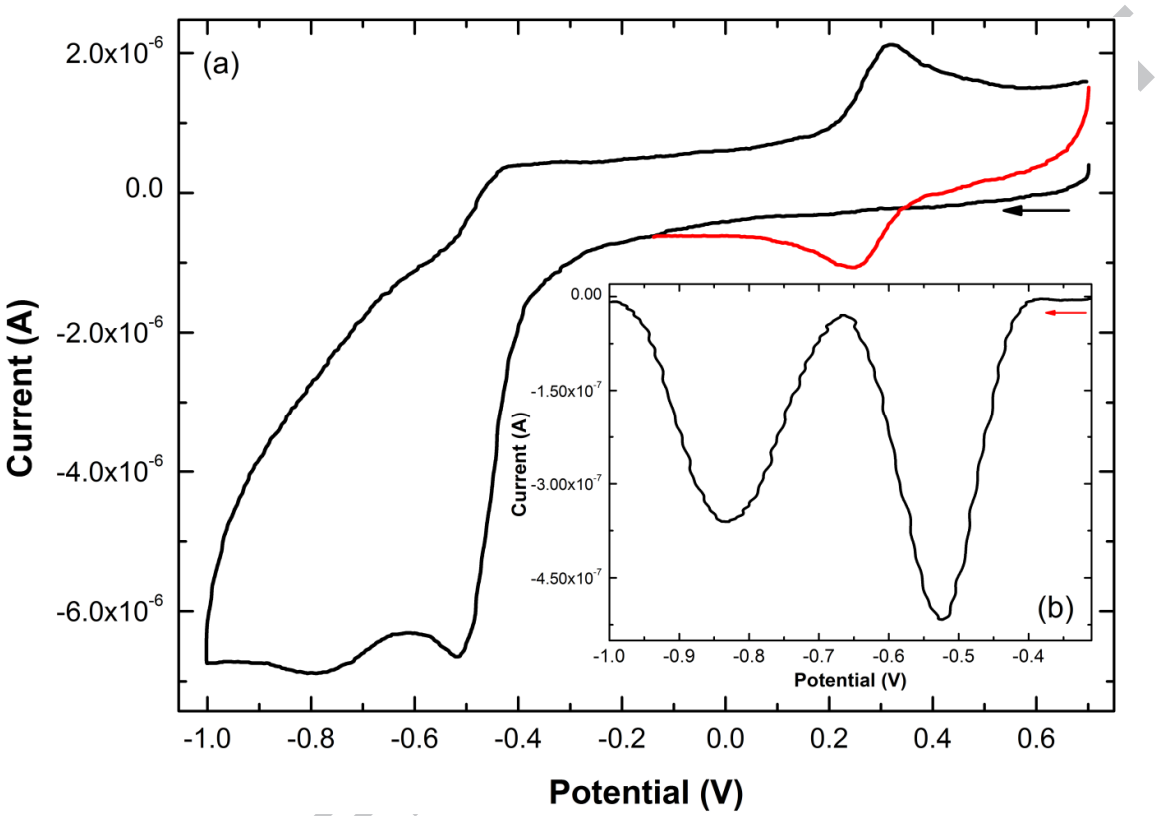

513

514 **Figure 2**

515

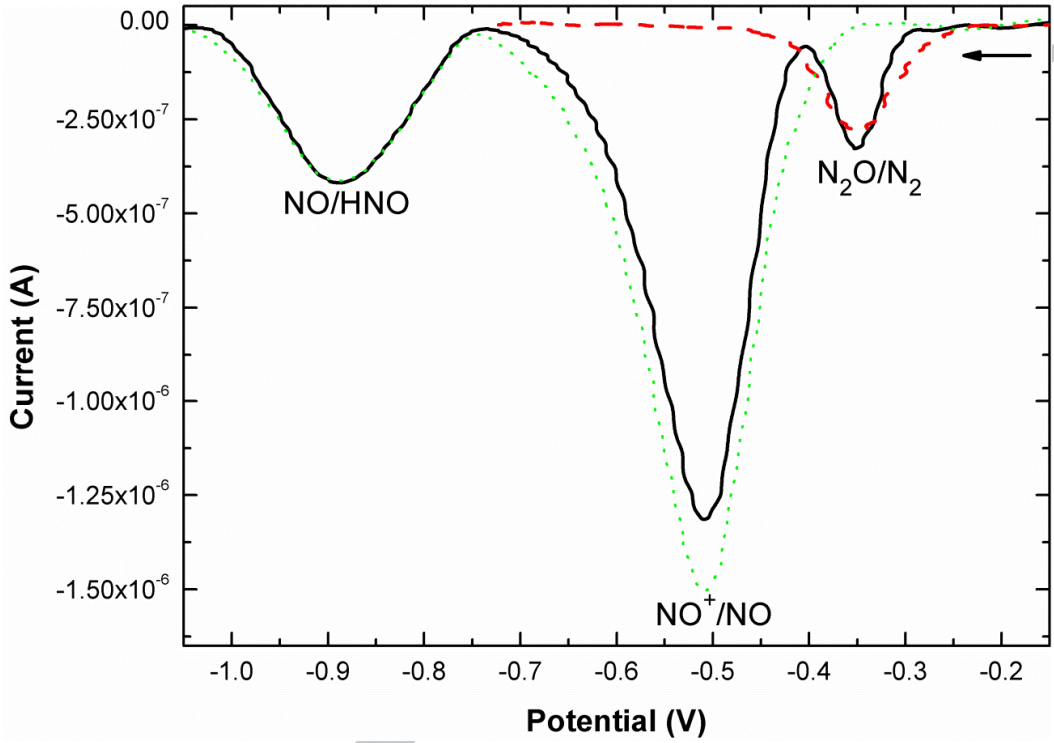

516

517

518

519 **Figure 3**

520

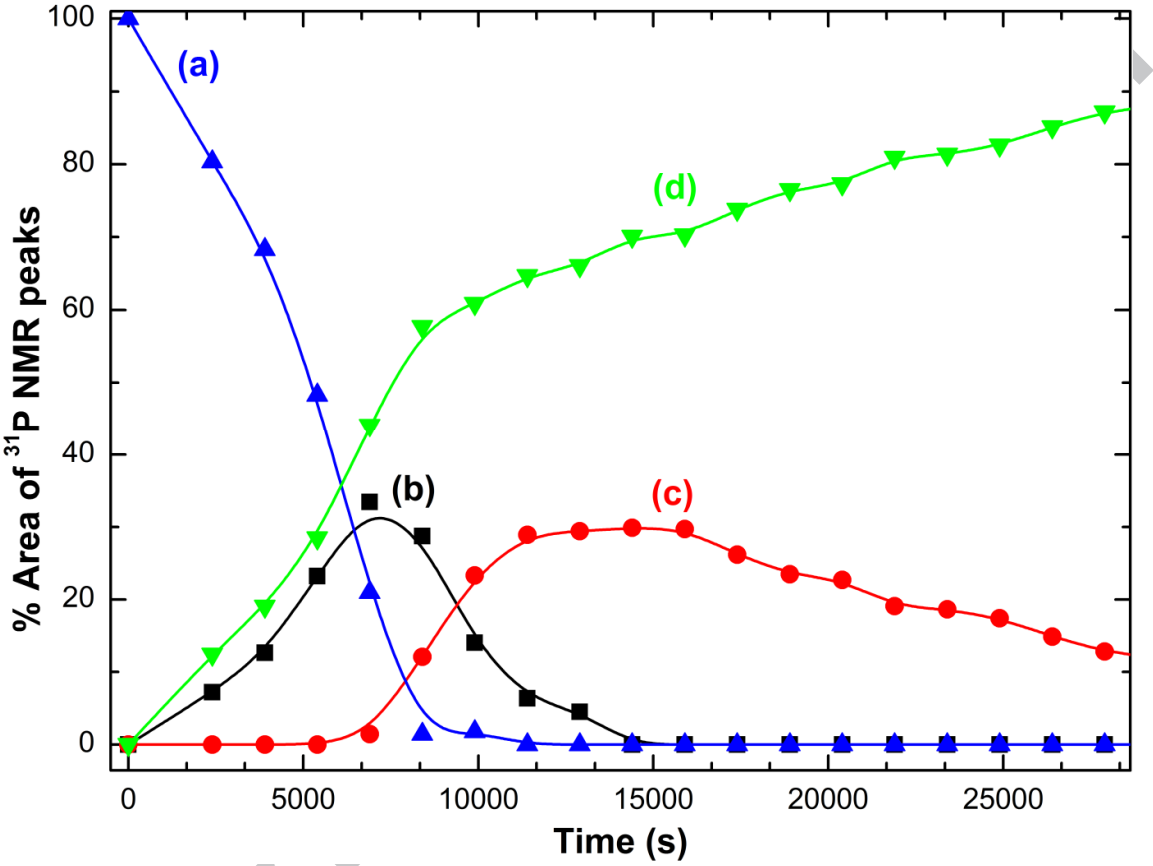

521

522

523

Figure 4

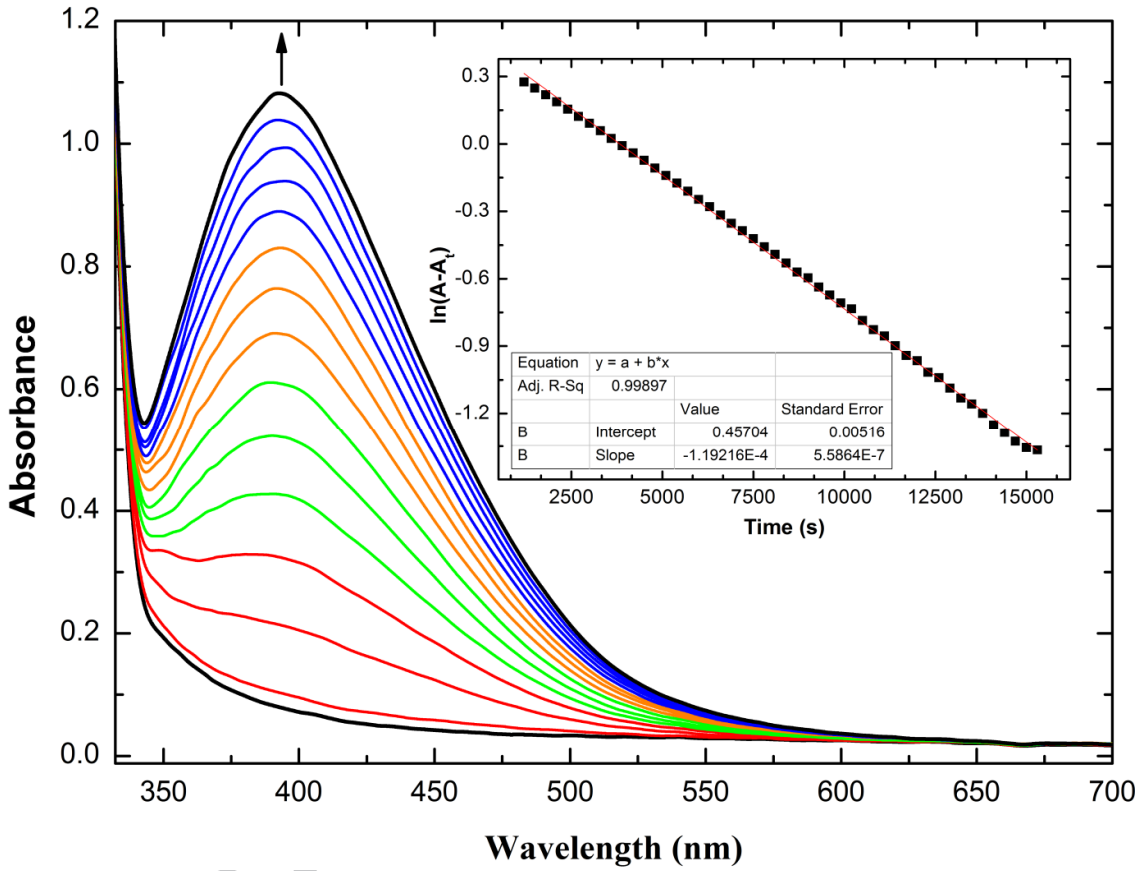

Table 1. NMR chemical shifts for *trans*-$[Ru(NO)(NH_3)_4P(O)(OEt)_2]^{2+}$ in D_2O using the TMSP-D4 and NH_4PF_6 as internal references.

Nuclei		Chemical Shift (ppm)
^{31}P		68.0
^{13}C	CH_2	65.3
	CH_3	18.8
^{1}H	CH_2	4.14
	CH_3	1.30

Graphical Abstract

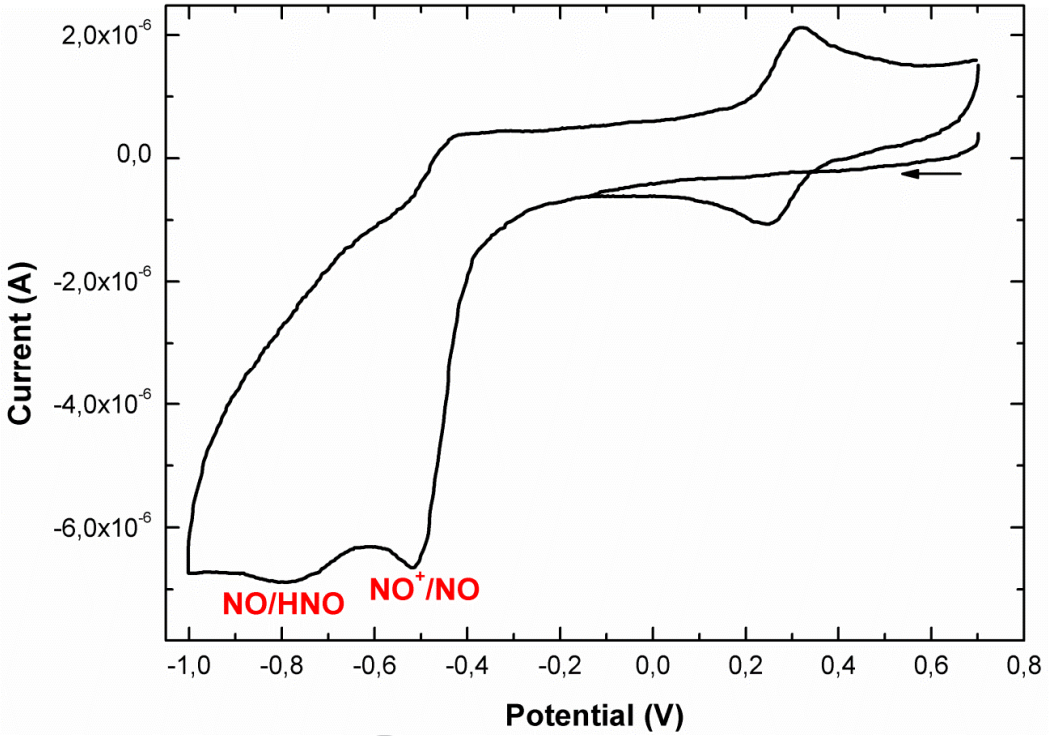

Graphical Abstract

The synthesis and the reactivity in aqueous media of the new compound *trans*-$[Ru(NO)(NH_3)_4P(O)(OEt)_2](PF_6)_2$ are described. This compound is a potentially good NO/HNO-donor in biological media due to its remarkable robustness over a wide pH range and exhibits a fast NO/HNO release when activated through one or two electrons reduction. Preliminary *in vivo* tests indicate that this complex reduces pain perception

553 ***Highlights***

554

555 • The reactivity of the new *trans*-$[Ru(NO)(NH_3)_4P(O)(OEt)_2](PF_6)_2$ in aqueous medium
556 is reported.

557 • This compound is a potential NO/HNO-donor upon electrochemical activation.

558 • It is stable in aqueous media over a wide pH range.

559 • *Trans*-$[Ru(NO)(NH_3)_4P(O)(OEt)_2]^{2+}$ decays with a half-life of 1.5 h at pH 7.5 and
560 25°C.

561

562